Manuscript Ref.: KIN-16-0118 (Revised)

Two Rate-Constant Kinetic Model for the Chromium(III)-EDTA Complexation Reaction by Numerical Simulations

JOAQUIN F. PEREZ-BENITO

Departamento de Ciencia de Materiales y Quimica Fisica, Sección de Quimica Fisica, Facultad de Quimica, Universidad de Barcelona, Marti i Franques, 1, 08028 Barcelona, Spain

---

Correspondence to: J. F. Perez-Benito; e-mail: jfperezdebenito@ub.edu.

Supporting Information is available in the online issue at www.wileyonlinelibrary.com.

ABSTRACT: The complexation reaction of Cr(III) ion in the presence of a large excess of EDTA does not follow a pseudo-first-order kinetics as sometimes suggested. There are two causes for the deviation from this simple behavior: the involvement of a long-lived intermediate, precluding the application of the steady-state approximation, and the autoinhibition provoked by the release of hydrogen ions from the organic ligand to the medium as the final Cr(III)-EDTA violet complex is formed. Numerical simulations have allowed obtaining for each kinetic experiment the values of two rate constants, k_1 (corresponding to the formation of the long-lived intermediate from the reactants) and k_2 (corresponding to the formation of the final complex product from the long-lived intermediate), as well as the number of hydrogens liberated per molecule of final complex product formed (H_{kin}). The results indicate that k_1 is associated to a fast step (E_a = 87 ± 4 kJ mol^{-1}) and k_2 to a slow step (E_a = 120 ± 2 kJ mol^{-1}), whereas the number of hydrogen ions lies within the range $0 < H_{kin} < 2$ in all the kinetic runs. A mechanism in accordance with the experimental data has been proposed.

INTRODUCTION

In most kinetic studies found in the chemical literature the reactions are reported to be of pseudo-first-order (after application of the isolation method). However, it should be emphasized that the concept of kinetic order can be applied only in particular cases in which the kinetic behavior is simple enough to be described by the use of a single pseudo-rate constant. When fitting of the concentration-time plots requires the use of two or more pseudo-rate constants, the classification of the reaction according to its presumed kinetic order might lead to erroneous conclusions. It is described here an important example where this has occurred: the complexation reaction of chromium(III) by ethylenediaminetetraacetic acid (EDTA).

Chromium(III) is an important species both in the chemistry laboratory and in biology. In the first case, it is the final product from nearly all chromium(VI) oxidations of different reducing agents [1,2]. In the second, it is a trace element required in the formation of the glucose tolerance factor (GTF) by coordination with a peptide molecule and playing a central role in the cellular carbohydrate metabolism [3,4]. In addition, Cr(III) complexes with several biological ligands showing GTF-like activity have been prepared [5]. Although Cr(III) supplementation has been proposed as a potential therapy to improve insulin sensitivity in diabetic patients [6], intoxication by this element has been described [7]. An interesting result reported in the scientific literature is that Cr(III) leads to notable increases in both median and maximum lifespan in rodents [8]. The effects of supplemental Cr(III) are similar to those observed in animals on calorie-restricted diets: decreased glucose levels, enhanced insulin sensitivity, and longer lifespan [9].

On the other hand, EDTA is a useful chemical substance exhibiting both reducing [10,11] and complexing [12 – 14] reactivities. Among the latter, its ability to complex divalent [15,16]

and trivalent [17 – 19] metal ions as a polydentate ligand is noteworthy. For instance, it can be used to complex Fe(II) and Fe(III) ions in kinetic studies of the Fenton reaction [20,21], as well as a food additive to trap metal impurities [22]. The metal-chelating character of EDTA makes it helpful as a therapy in intoxications by metal ions [23]. In particular, it has been used for the treatment of Wilson's disease (copper overload) [24] and thalassemia (iron overload) [25] patients. Actually, EDTA-chelating therapy for the treatment of metal-induced diseases has already been applied in millions of patients [26]. In addition, its applications have recently been extended to the nanomedicine field [27].

The chemical structure of the Cr(III)-EDTA complex has been the objective of some spectroscopic research [28 – 30] and quantitative determinations of its acid-base properties have also been reported [31]. This complexation has been applied to the elimination of toxic and carcinogenic Cr(VI) by ultrafiltration techniques [32]. The kinetics of the reactions of Cr(III) with EDTA and similar ligands [33,34] have been studied both in the absence and in the presence of hydrogen peroxide [35,36]. Although the Cr(III)-EDTA reaction under conditions of a large ligand/metal excess has so far been classified as a pseudo-first-order reaction [37 – 39], some experimental results showing compelling evidence of deviations from this simple kinetic behavior have been found and will be presented here forth.

EXPERIMENTAL

Materials and Methods

The solvent used in all the experiments was water previously purified by deionization followed by treatment with a Millipore Synergy UV system (milli-Q quality, κ = 0.05 μS/cm at 25.0 ºC). The reactants used in all the experiments were chromium(III) nitrate nonahydrate [$Cr(NO_3)_3 \cdot 9H_2O$, Merck, purity ≥ 98.0%] and sodium dihydrogen ethylenediaminetetraacetate dihydrate [$(NaOOCCH_2)_2NCH_2CH_2N(CH_2COOH)_2 \cdot 2H_2O$, Na_2EDTA, Panreac, purity ≥ 99.0%]. When necessary, in some experiments other reactants were also added: potassium hydroxide (KOH, Merck, purity ≥ 85%), potassium nitrate (KNO_3, Merck, purity ≥ 99.0%), gum arabic (Merck), polyvinylpyrrolidone [$(C_4H_6ONCHCH_2)_n$, PVP, Sigma-Aldrich] and the organic solvents (Sigma-Aldrich, purity ≥ 99.0%) methanol (CH_3OH), ethanol (CH_3CH_2OH), 1-propanol ($CH_3CH_2CH_2OH$), 2-propanol ($CH_3CHOHCH_3$), 1-butanol ($CH_3CH_2CH_2CH_2OH$), ethylene glycol (CH_2OHCH_2OH) and acetone (CH_3COCH_3).

The pH measurements were done by means of a Metrohm 605 pH-meter, provided with a digital presentation until the third decimal figure (± 0.001 pH) and a combination electrode, calibrated with the aid of two commercial buffers at pH 4.00 ± 0.02 and 7.00 ± 0.01 (Sigma-Aldrich). The temperature was kept constant by means of a Julabo thermostatic bath provided with a digital reading (± 0.1 ºC). The absorbances were measured and the spectra recorded with a Shimadzu 160 A UV-Vis spectrophotometer (± 0.001 A). Quartz cuvettes (optical path length: 1 cm) were used. The kinetic runs were followed at five different wavelengths (410, 445, 495, 540 and 575 nm), measuring the absorbances periodically at time intervals of 180 – 360 s.

Kinetic Experiments

In most of the runs the initial concentration of the complexing agent, Na_2EDTA, was much higher than that of the metallic ion, Cr(III), in order to attain an approximately constant concentration of the organic reactant (isolation method). The total solution volume was kept the same in all the experiments (51 mL). Among the five wavelengths chosen to monitor the process, 540 nm corresponded to the maximum increase of the solution absorbance during the course of the reaction and, to minimize the experimental errors, was chosen to obtain the kinetic data. In order to assess reproducibility, all the runs were duplicated.

Kinetic Calculations

A program was written in BASIC language for the treatment of the absorbance-time experimental data. Four fitting parameters were required: the initial absorbance (A_o), the number of hydrogen ions released per Cr(III)-EDTA complex molecule formed (H_{kin}) and two pseudo-rate constants (k_1 and k_2). Pseudo-rate constant k_1 was associated to the conversion of the reactant Cr(III) into a long-lived intermediate, whereas k_2 was associated to the base-catalyzed decay of that intermediate to yield the final complex product. The calculations were implemented on a Sony Vaio personal computer.

RESULTS AND DISCUSSION

The reaction was studied in the absence of an added buffer in order to avoid any perturbation caused by the competition of its anionic form with EDTA as a Cr(III) potential ligand. Although EDTA actually exercised some self-buffering action, the retarding effect caused by the decrease in pH as the reaction advanced allowed obtaining some valuable information on the number of hydrogen ions released to the medium during the formation of different Cr(III)-EDTA complexes.

Electronic Spectra

A periodical scanning of the UV-Vis spectrum of the solution during the course of the reaction is shown in Fig. 1 (top). It can be seen that the absorbance increased with time over the whole wavelength range, and that the peaks corresponding to the violet complex product (392 and 540 nm) were shifted toward the left with respect to those corresponding to the blue-gray complex reactant (412 and 576 nm). Moreover, whereas for the reactant $[Cr(H_2O)_6]^{3+}$ the low-wavelength band was more pronounced than the high-wavelength band, for the product Cr(III)-EDTA happened the opposite. No isosbestic point was observed.

Involvement of a Long-Lived Intermediate

In the present case, there are at least two chemical species absorbing light in the visible region of the spectrum: the reactant $[Cr(H_2O)_6]^{3+}$ and the product Cr(III)-EDTA. When a reaction is followed spectrophotometrically at two different wavelengths (λ_1 and λ_2) at which both the

reactant (R) and the product (P) absorb light, assuming that the Lambert-Beer law is fulfilled and that all the intermediates involved in the mechanism are short lived (in steady state), it is easy to demonstrate that the relationship between the corresponding absorbances $A(\lambda_1)_t$ and $A(\lambda_2)_t$ at time *t* should be:

$$A(\lambda_1)_t = A(\lambda_1)_o + \frac{\varepsilon_{P,1} - \varepsilon_{R,1}}{\varepsilon_{P,2} - \varepsilon_{R,2}} \left[A(\lambda_2)_t - A(\lambda_2)_o \right] \quad (1)$$

where $A(\lambda_1)_o$ and $A(\lambda_2)_o$ are the initial absorbances at the two wavelengths, whereas the subscripts of the molar absorption coefficients indicate the corresponding species and wavelength. Hence, provided that the above mentioned hypotheses are fulfilled, an $A(\lambda_1)$ vs $A(\lambda_2)$ plot is expected to be linear. A representation of the absorbance at 445 nm versus the absorbance at 540 nm during the course of the reaction for a typical kinetic experiment is shown in Fig. 1 (bottom). These wavelengths were selected because the visible spectrum of the final Cr(III)-EDTA complex had a minimum at the first (445 nm) and maximum at the second (540 nm). Thus, the existence of an absorption minimum for the product at 445 nm offered a chance to look for any absorption caused by a potential long-lived intermediate. The plot shows a definite upward-concave curvature instead of the expected linearity. Since, of the conditions required for fulfilment of Eq. (1), the validity of the steady-state approximation for all the intermediates is the one with a higher probability of not being reached, the curvature of the *A*(445) vs *A*(540) plot suggests that a long-lived intermediate is involved in the reaction mechanism. This hypothesis was confirmed later by the excellent agreement between the absorbance-time experimental data and the numerical simulations based on it.

Formation of Two Cr(III)-EDTA Complexes

The absorbance measured at 540 nm at the end of the process increased with the initial Cr(III) concentration (Fig. 2, top). However, the relationship was not exactly linear, since it showed a certain downward-concave curvature, indicating that the optical behavior of the violet complex formed as product exhibited some deviation with respect to that predicted by the Lambert-Beer law. Although other explanations are indeed feasible, this deviation would be consistent with the coexistence of two Cr(III)-EDTA complexes with different metal/ligand stoichiometric ratios. When EDTA was in large excess with respect to Cr(III) (at low initial metal ion concentration) the 1:2 complex would be predominant whereas when the excess was lower (at high initial metal ion concentration) the contribution of the 1:1 complex would be increasingly important. According to this interpretation, the molar absorption coefficients would be in the sequence $\mathcal{E}_{540}(1{:}0) = 12\ M^{-1}\ cm^{-1} < \mathcal{E}_{540}(1{:}1) = 188\ M^{-1}\ cm^{-1}$ (upper limit) $< \mathcal{E}_{540}(1{:}2) = 230\ M^{-1}\ cm^{-1}$, the first of them corresponding to the hexaaquachromium(III) ion and the others to the 1:1 and 1:2 Cr(III)-EDTA complexes. The value of $\mathcal{E}_{540}(1{:}0)$ was obtained from the initial absorbance at 540 nm (before the violet complex is formed), whereas the upper limit for the value of $\mathcal{E}_{540}(1{:}1)$ and the value of $\mathcal{E}_{540}(1{:}2)$ were obtained from the slopes of the tangents to the curve shown in Fig. 2 (top) at the highest experimental value of $[Cr(III)]_o$ (lowest ligand/metal ratio) and at $[Cr(III)]_o = 0$ (infinite ligand/metal ratio), respectively. It was reported that the 1:1 complex still retains one water molecule in its coordination sphere [40], and the new data suggest that the 1:2 complex retains none. As a result, it can be concluded that successive replacement of Cr(III)-H_2O bonds by Cr(III)-EDTA bonds leads to an increase of the electronic absorption at 540 nm.

The final pH showed a singular profile when represented as a function of the initial Cr(III) concentration, showing first a definite decrease, passing through a minimum, increasing later and reaching a plateau at the end (Fig. 2, bottom). This plot suggests that the organic divalent ion (H_2Y^{2-}) used as initial reactant suffers a partial deprotonation during the formation of the complex and that the number of hydrogen ions released to the medium is higher for the 1:2 complex than for the 1:1 counterpart. In this way, the initial decrease of the pH_∞ vs $[Cr(III)]_o$ plot would correspond to the conditions for which the 1:2 complex predominates (high [ligand]/[metal] ratio), whereas the posterior increase and final plateau would correspond to the range for which the contribution of the 1:1 complex starts to be high enough (low [ligand]/[metal] ratio). Thus, we can conclude that the plots shown in Fig. 2 cannot be explained by the formation of just one Cr(III)-EDTA complex with a unique metal-ligand stoichiometric ratio, strongly suggesting that at least two complexes were formed.

One Rate-Constant Kinetic Model

In the literature, the Cr(III)-EDTA reaction in the presence of a ligand/metal large excess has been classified as a pseudo-first-order process [37–39]. The absorbance at 540 nm has been represented versus time for a typical kinetic run (Fig. 3, top) and it can be observed, however, that the plot shows a sigmoid profile, with an upward-concave curvature at the beginning followed by an inflection point and a downward-concave curvature at the end of the reaction. This behavior is quite different from the uniformly downward-concave plot expected for a pseudo-first-order reaction according to the exponential function:

$$A_t = A_\infty - (A_\infty - A_o)\, e^{-k t} \quad (2)$$

where A_o, A_t and A_∞ are the absorbances at the beginning, at time t and at the end of the reaction, respectively, whereas k is the pseudo-first-order rate constant.

Linearization of Eq. (2) yields:

$$\ln (A_\infty - A_t) = \ln (A_\infty - A_o) - k t \quad (3)$$

However, systematic deviations of the experimental data from the straight line were observed in the attempted pseudo-first-order plots for all the kinetic runs, presenting a downward-concave curvature at the beginning of the reaction and an upward-concave curvature at the end (Fig. 3, bottom).

On the other hand, for a pseudo-first order reaction an exponential decay of the reaction rate with time would be expected:

$$\nu_t = k\,[\mathrm{R}]_t = k\,[\mathrm{R}]_o\, e^{-k t} \quad (4)$$

where $[R]_o$ and $[R]_t$ are the concentrations of the limiting reactant, hexaaquachromium(III) ion, at the beginning of the reaction and at time t, respectively. However, the reaction rate vs time plots showed in all the cases a bell-shaped profile, with a definite acceleration period followed by a maximum and a deceleration period (Fig. 4, top). During the latter, a double-logarithm plot of the rate vs the total concentration of Cr(III) not present as reaction product (limiting reactant + long-lived intermediate) yielded a roughly straight line with slope 1.98 ±

0.03 (Fig. 4, bottom). The reaction rate values were obtained from the absorbance at 545 nm vs time kinetic data by means of a combination of the finite-difference method of derivation and the formula of physical additive properties as $v_{t+\Delta t/2} = (A_{t+\Delta t} - A_t)[\mathrm{Cr(III)}]_o/[(A_\infty - A_o)\Delta t]$ for small values of Δt.

Thus, the experimental behavior revealed two distinct deviations from the simple pseudo-first-order kinetic model: an initial acceleration period, as well as a posterior deceleration period where the reaction rate decreased much faster than expected for a pseudo-first-order reaction. These deviations were probably originated by two independent causes, and led to the conclusion that a new and more elaborated kinetic model was required.

Two Rate-Constant Kinetic Model

Many different mechanisms were tried by numerical simulations until finding one leading to good results. The experimental absorbance-time data were consistent with the simplified mechanism given by the following sequence:

$$\mathrm{R} \xrightarrow{k_1} \mathrm{I} \xrightarrow[\mathrm{HO^-}]{k_2} \mathrm{P} \qquad (5)$$

where R is the limiting reactant, $[Cr(H_2O)_6]^{3+}$, I the long-lived intermediate, P the Cr(III)-EDTA final product, k_1 the pseudo-first-order rate constant for the first step and k_2 the pseudo-second-order rate constant for the base-catalyzed second step. The corresponding differential equations are:

$$\frac{\mathrm{d[R]}}{\mathrm{d}t} = -k_1\,[\mathrm{R}] \tag{6}$$

$$\frac{\mathrm{d[I]}}{\mathrm{d}t} = k_1\,[\mathrm{R}] - k_2\,[\mathrm{I}]\,[\mathrm{HO^-}] \tag{7}$$

$$\frac{\mathrm{d[P]}}{\mathrm{d}t} = k_2\,[\mathrm{I}]\,[\mathrm{HO^-}] \tag{8}$$

Equations (6)-(8) have been integrated for each kinetic experiment by means of a numerical approximate procedure, the fourth order Runge-Kutta method [41]. In this way, once known the initial concentration of R, as well as those of I and P (both equal to 0), the concentrations of the three species at different instants during the course of the reaction could be obtained, using to that end short time intervals (Δt = 180 – 360 s, depending on the experimental conditions). The concentration of hydroxide ion during the course of the reaction was obtained from a combination of the EDTA dissociation equilibrium constants and the number of hydrogen ions released per Cr(III)-EDTA complex formed. As a starting point, a BASIC computer program (KIN SIM, Supporting Information) was developed for the optimization of the values of the 5 fitting parameters involved: the initial absorbance (A_o), the number of hydrogen ions released during the reaction (H_{kin}), the two pseudo-rate constants (k_1 and k_2) and the ratio between the molar absorption coefficients of the inorganic reactant and the long-lived intermediate at 540 nm (Q). Different combinations of those parameters were systematically tried for each kinetic run until reaching a minimum of the average error defined as:

$$E = \frac{\sum_{i=1}^{N} \left| A_{i,cal} - A_{i,exp} \right|}{N} \tag{9}$$

where $A_{\lambda,cal}$ and $A_{\lambda,exp}$ are the calculated and experimental absorbances, respectively, and N is the number of time-absorbance datum couples for each kinetic run. The average value found for the ratio of molar absorption coefficients corresponding to 28 kinetic runs with different initial concentrations of metal ion and organic ligand was $Q = 0.98 \pm 0.04$ (Table I). The fact that this value is so close to unity suggests that the number of Cr(III)-EDTA chemical bonds in the long-lived intermediate is much lower than in the final complex product, probably just one bond. In order to decrease the accidental errors associated to the kinetic parameters, the numerical simulations were performed for all the kinetic experiments with 4 fitting parameters, taking $Q = 1$ (the same molar absorption coefficients for the inorganic reactant and the long-lived intermediate). The values of A_o obtained from the fits were consistent within the experimental errors with the ones measured for the same concentrations of Cr(III) in the absence of EDTA.

Comparison between Kinetic Models

The values of the average error were within the ranges $E = 3.46 \times 10^{-3} - 3.67 \times 10^{-2}$ for the one rate-constant model and $E = 2.90 \times 10^{-4} - 1.40 \times 10^{-3}$ for the two rate-constant model, indicating that the errors between calculated and experimental absorbances were one order of magnitude smaller in the second case. This was confirmed by representing the ratio between the calculated (according to the two kinetic models) and experimental absorbances at 540 nm as a function of time for a typical kinetic run (Fig. 5). The values were within the ranges $A(540)_{cal}/A(540)_{exp} = 0.953 - 1.640$ for the one rate-constant model and $A(540)_{cal}/A(540)_{exp} = 0.989 - 1.007$ for the two rate-constant model. Moreover, the plot showed only 2 crossing

points with the horizontal line of $A(540)_{cal}/A(540)_{exp} = 1$ (corresponding to a perfect fit) for the one rate-constant model and 52 crossing points for the two rate-constant model, indicating that the errors were essentially of systematic nature in the first case and of accidental nature in the second. It can then be concluded that the two rate-constant model is a better choice to describe the kinetic behavior of the Cr(III)-EDTA complexation reaction than the one rate-constant model.

Time Evolution of the Cr(III) Complexes

The concentration vs time profiles for the limiting reactant, the long-lived intermediate and the final product, calculated according to the two rate-constant model, have been plotted for a typical kinetic run in Fig. 6 (top). It can be seen that the formation of the intermediate from the reactant was rather fast, whereas the formation of the product from the intermediate was much slower. A comparison of the experimental reaction rate with the calculated long-lived intermediate concentration (Fig. 6, bottom) revealed that the initial increase of the rate almost exactly matched the increase of the intermediate concentration. However, the maximum in the rate took place slightly before than the maximum in the intermediate concentration, and the rate decreased much faster than the concentration. This fast deceleration was caused (according to the proposed kinetic model) by the decrease in the solution pH due to the release of hydrogen ions during the reaction.

Number of Hydrogen Ions Released

In order to form its complex with Cr(III), the dianionic form of EDTA must lose at least part of its acidic hydrogen atoms. The number of hydrogen ions released per Cr(III)-EDTA complex molecule formed has been denoted as H. The value of this parameter corresponding to each experiment was obtained in two different ways: from the fitting of the absorbance-time data (kinetic value, H_{kin}) and from the measurements of the pH values at the end of the reaction combined with the acidity equilibrium constants reported in the literature [42] for the dissociations of H_3Y^- and H_2Y^{2-} (thermodynamic value, H_{th}). Both H_{kin} and H_{th} decreased as the metal ion initial concentration increased, and their respective values converged at high $[Cr(III)]_o$ (Fig. 7, top). On the contrary, an increase in the initial ligand concentration led to an increase of both H_{kin} and H_{th}, and their respective values converged at low $[Na_2EDTA]_o$ (Fig. 7, middle). Addition of KOH resulted in an increase of both H_{kin} and H_{th} (Fig. 7, bottom). The values found for these parameters were in the range $0 < H < 2$ in all the experiments, with a trend to $H_{th} > H_{kin}$.

Kinetic Data

Excellent accordance between the experimental absorbances and those predicted by the two rate-constant kinetic model was observed in all the kinetic runs (see Fig. 8).

After application of the isolation method, the pseudo-rate constants should be independent of the initial concentration of the limiting reactant. Thus, this independence can be adopted as a criterion to check the validity of the kinetic model used to fit the experimental data. In the present case, pseudo-rate constant k_1 was independent of the initial concentration of metal

ion, whereas k_2 decreased as that concentration increased (Table II). A double-logarithm plot of k_1 vs $[Cr(III)]_o$ yielded the slope 0.04 ± 0.03, whereas that of k_2 yielded the slope – 0.27 ± 0.03. The small absolute values of those slopes indicated that the two rate-constant model, although not perfect (especially as concerning the determination of k_2), was a rather faithful description of the kinetics followed by the Cr(III)-EDTA complexation reaction.

Both pseudo-rate constants increased with increasing initial ligand concentration, although the dependence of k_1 on $[EDTA]_o$ (Fig. 9, top) was stronger than that of k_2 (Fig. 9, bottom). The experimental data could be fitted to the functions:

$$k_1 = \frac{a_1 [EDTA]_o}{1 + b_1 [EDTA]_o} \quad (10)$$

$$k_2 = \frac{a_2 [EDTA]_o}{1 + b_2 [EDTA]_o} + c_2 \quad (11)$$

with $a_1 = (3.8 \pm 0.2) \times 10^{-2}$ M^{-1} s^{-1}, $b_1 = 14 \pm 2$ M^{-1}, $a_2 = (7.4 \pm 0.2) \times 10^{6}$ M^{-2} s^{-1}, $b_2 = 26.0 \pm 1.2$ M^{-1} and $c_2 = (4.02 \pm 0.12) \times 10^{4}$ M^{-1} s^{-1}. Thus, it can be concluded that, although EDTA is a reactant essential in the part of the mechanism associated to pseudo-rate constant k_1, in that associated to pseudo-rate constant k_2 there are at least two reaction pathways involved, one including EDTA as a reactant and the other not (see that, for $[EDTA]_o = 0$, $k_1 = 0$ and $k_2 = c_2$).

The reaction showed base catalysis. Pseudo-rate constant k_1 increased linearly with increasing $[KOH]_o$ (Fig. 10, top), whereas k_2 decreased at first and reached soon a plateau

(Fig. 10, bottom). Addition of KNO_3 resulted in slight changes of the pseudo-rate constants, a decrease of k_1 and an increase of k_2, whereas the value of H_{kin} increased (Table III).

Addition of the water-soluble polymer polyvinylpyrrolidone (PVP) did not appreciably change the values of either k_1, k_2 or H_{kin} (Table S1, Supporting Information). Since PVP was expected to act as a protective colloid, hindering the approach of EDTA to a potential Cr(III) intermediate species of colloidal nature, its lack of noticeable effect on the rate of the Cr(III)–EDTA reaction allows to exclude colloidal $Cr(OH)_3$ as a possible intermediate in the mechanism of this complexation process. However, when the water-soluble polymer gum arabic (GA) was added, a net decrease in all k_1, k_2 and H_{kin} was observed (Table S2, Supporting Information). This suggests the possible formation of a complex between Cr(III) and the polysaccharide GA in competition with the Cr(III)-EDTA complexation reaction. Actually, the monosaccharide D-ribose is known to form long-lived intermediate complexes in its reaction with Cr(VI) [43,44].

Addition of an organic solvent (several alcohols or acetone) resulted in an increase of both pseudo-rate constants k_1 (Fig. 11, top) and k_2 (Fig. 11, bottom), with the only exception of 1-butanol (which led to a decrease of k_2). The results shown in Table IV for the slopes of the log ($k_1/k_{1,0}$) vs [organic solvent]$_o$ and log ($k_2/k_{2,0}$) vs [organic solvent]$_o$ linear plots ($k_{1,0}$ and $k_{2,0}$ being the pseudo-rate constants in the absence of organic solvent) indicate that in the homologous series of primary alcohols the rate-increasing effect followed the sequence of increasing non-polar hydrocarbon chain length (methanol < ethanol < 1-propanol < 1-butanol) as far as k_1 was concerned. Moreover, the slopes of the log ($k_1/k_{1,0}$) vs [organic solvent]$_o$ linear plots were strongly correlated with the number of carbon atoms in the hydrocarbon chain for all the 7 organic solvents studied (Fig. 12). However, the effect on k_2 was rather similar for the different solvents (1-butanol excepted). A comparison of the data shown in

Tables IV and S3 (Supporting Information) reveals that an increase of the initial EDTA concentration resulted in a net decrease of the ethanol effect on k_1 (duplication of that concentration led to a decrease of the slope from 0.124 ± 0.006 M^{-1} to 0.048 ± 0.005 M^{-1}) whereas the effect on k_2 remained unchanged (0.081 ± 0.009 M^{-1} vs 0.078 ± 0.010 M^{-1}, respectively).

The fulfilment of the Arrhenius equation was reasonably good for k_1 (Fig. 13, top) and excellent for k_2 (Fig. 13, bottom). The activation energy associated to the second pseudo-rate constant was much higher than that associated to the first (Table V). Although the activation entropy corresponding to k_1 was slightly negative and that corresponding to k_2 largely positive, caution should be exercised when interpreting these results, for it has to be reminded that activation entropies associated to pseudo-rate constants with different units cannot be compared, since they present a different dependence on the arbitrary choice of the standard state [45].

Mechanism

According to the experimental information so far available, the mechanism that can be proposed for the Cr(III)-EDTA complexation reaction can be divided into two different sections, each corresponding to one of the pseudo-rate constants. The elementary steps associated to the first constant are the following:

$$[Cr(H_2O)_6]^{3+} + H_2Y^{2-} \overset{K_I}{\rightleftharpoons} [Cr(H_2O)_6]^{3+} - H_2Y^{2-} \qquad (12)$$

$$[Cr(H_2O)_6]^{3+} - H_2Y^{2-} + HO^- \overset{K_{II}}{\rightleftharpoons} [Cr(HO)(H_2O)_5]^{2+} - H_2Y^{2-} + H_2O \qquad (13)$$

$$[Cr(H_2O)_6]^{3+} - H_2Y^{2-} \xrightarrow[\text{slow}]{k_{III}} [Cr(H_2Y)(H_2O)_5]^{+} + H_2O \qquad (14)$$

$$[Cr(HO)(H_2O)_5]^{2+} - H_2Y^{2-} \xrightarrow[\text{slow}]{k_{IV}} [Cr(H_2Y)(H_2O)_5]^{+} + HO^- \qquad (15)$$

An inorganic-organic ion pair is proposed to be reversibly formed in Eq. (12) from hexaaquachromium(III) ion and the dianionic form of EDTA predominant in the medium. This section of the mechanism involves two different rate-determining (slow) steps for the two reaction pathways involved (without base catalysis and with it). The proposed long-lived intermediate [chemical species I in Eq. (5)] is the Cr(III) complex formed in Eqs. (14) and (15).

Since Eq. (12) does not involve the breaking of any Cr(III)-H_2O chemical bond, it is expected to be fast enough to be in quasi-equilibrium. The same can be stated about Eq. (13), corresponding to a fast, reversible acid-base reaction. Thus, application of the quasi-equilibrium approximation to those steps leads to the following laws for the first part of the mechanism:

$$v_1 = k_1 [Cr(H_2O)_6^{3+}] \qquad (16)$$

$$k_1 = \frac{K_I [EDTA]}{1 + K_I [EDTA]} \left(k_{III} + K_{II} k_{IV} [HO^-]\right) \qquad (17)$$

Equation (17) is consistent with the kinetic results shown in Figs. 8 (top) and 9 (top), as well as with Eq. (10) provided that $a_1 = K_I \left(k_{III} + K_{II} k_{IV} [HO^-]\right)$ and $b_1 = K_I = 14 \pm 2\ M^{-1}$.

For the mechanism associated to the second pseudo-rate constant the following elementary steps can be proposed:

$$[Cr(H_2Y)(H_2O)_5]^+ + HO^- \overset{K_V}{\rightleftharpoons} [Cr(HO)(H_2Y)(H_2O)_4] + H_2O \quad (18)$$

$$[Cr(HO)(H_2Y)(H_2O)_4] + H_2Y^{2-} \overset{K_{VI}}{\rightleftharpoons} [Cr(HO)(H_2Y)(H_2O)_4]-H_2Y^{2-} \quad (19)$$

$$[Cr(HO)(H_2Y)(H_2O)_4] \xrightarrow[\text{slow}]{k_{VII}} [Cr(H_2Y)(H_2O)_2]^+ + HO^- + 2H_2O \quad (20)$$

$$[Cr(HO)(H_2Y)(H_2O)_4]-H_2Y^{2-} \xrightarrow[\text{slow}]{k_{VIII}} [Cr(HY)_2]^{3-} + H_3O^+ + 4H_2O \quad (21)$$

$$[Cr(H_2Y)(H_2O)_2]^+ \rightleftharpoons [Cr(HY)(H_2O)_2] + H^+ \quad (22)$$

$$[Cr(HY)(H_2O)_2] \xrightarrow[\text{slow}]{} [Cr(HY)(H_2O)] + H_2O \quad (23)$$

The long-lived intermediate previously formed suffers a fast acid-base reaction resulting in its deprotonation to yield a hydroxo complex [Eq. (18)]. The latter reacts in a reversible fast step with the dianionic form of EDTA to yield an adduct [Eq. (19)]. Two rate-determining steps are involved also in this part of the mechanism, leading to 1:1 [Eq. (20)] and 1:2 [Eq. (21)] complexes. The mechanism ends with a fast deprotonation of the 1:1 complex [Eq. (22)] followed by a slow reaction in which a water molecule is lost [Eq. (23)].

Both Eqs. (18) and (19) correspond to reversible reactions fast enough (the first acid-base and the second without involving the breaking of any bond other than the weak reactant-solvent intermolecular forces) for the quasi-equilibrium approximation to apply, leading to the following laws for the second part of the mechanism:

$$v_2 = k_2 [I] [HO^-] \quad (24)$$

$$k_2 = \frac{K_V}{1 + K_V [HO^-]} \left(k_{VII} + \frac{K_{VI} k_{VIII} [EDTA]}{1 + K_{VI} [EDTA]} \right) \quad (25)$$

where I ≡ $[Cr(H_2Y)(H_2O)_5]^+$ is the long-lived intermediate. Equation (25) is consistent with the kinetic results shown in Figs. 8 (bottom) and 9 (bottom), as well as with Eq. (11) provided that $a_2 = K_V K_{VI} k_{VIII} / (1 + K_V [HO^-])$, $b_2 = K_{VI} = 26.0 \pm 1.2$ M^{-1} and $c_2 = K_V k_{VII} / (1 + K_V [HO^-])$.

The decrease of rate constant k_1 with increasing ionic strength (Table III) can be explained by the effect on equilibrium constant K_I, expected to decrease because the corresponding reaction, Eq. (12), involves the encounter of two strongly charged anion-cation reactants. However, this decreasing effect failed to show up in the case of rate constant k_2, probably because the reaction associated to equilibrium constant K_V, Eq. (18), involves two ionic reactants with a much lower electrostatic charge, and the combined effects on the different elementary reactions should then be taken into account.

The number of hydrogen ions released to the medium during the reaction per Cr(III)-EDTA complex formed can be calculated as:

$$H_{kin} = \frac{[Cr(HY)(H_2O)] + 2 [Cr(HY)_2^{3-}]}{[Cr(H_2Y)(H_2O)_2^+] + [Cr(HY)(H_2O)] + [Cr(HY)_2^{3-}]} \quad (26)$$

where the concentration of $[Cr(HY)(H_2O)_2]$ has been neglected. It has been considered that per each $[Cr(H_2Y)(H_2O)_2]^+$, $[Cr(HY)(H_2O)]$ or $[Cr(HY)_2]^{3-}$ formed 0, 1 or 2 hydrogen ions are released to the medium, respectively. Equation (26) predicts that $0 < H_{kin} < 2$, in agreement

with the results shown in Tables II and III, as well as in Fig. 7. Moreover, an increase of $[Cr(III)]_o$ should result in an increase of the ratio of the 1:1 complexes (releasing either 0 or 1 hydrogen ions) versus the 1:2 complex (releasing 2 hydrogen ions), thus decreasing H_{kin}, what agrees with the results shown in Fig. 7 (top). On the contrary, an increase of $[EDTA]_o$ should result in an increase of the ratio of the 1:2 complex versus the 1:1 complexes, thus increasing H_{kin}, what agrees with the results shown in Fig. 7 (middle). Addition of KOH shifts the quasi-equilibrium defined by Eq. (22) toward the right side, thus increasing H_{kin}, in agreement with Fig. 7 (bottom). Furthermore, the trend observed for the value of the number of hydrogen ions liberated per Cr(III)-EDTA complex formed as calculated from the final experimental pH being higher than that calculated from the numerical simulations performed on the absorbance-time data ($H_{th} > H_{kin}$) can be explained by the combination of Eqs. (22) and (23) as long as the latter reaction is slow enough to have a negligible effect during the kinetic runs but a measurable effect on the final pH.

The effect of addition to the medium of low-polarity organic solvents is also consistent with the proposed mechanism. Given that Eq. (12) involves the participation as reactants of a strongly charged anion-cation pair, a decrease of the medium polarity is expected to result in an increase of equilibrium constant K_I and, hence, also of pseudo-rate constant k_1 [see Eq. (17)], because an enhancement of the anion-cation electrostatic attraction would produce an increase of the forward rate constant, the backward rate constant remaining essentially unchanged. However, since Eq. (18) involves as reactants a less strongly charged anion-cation pair, the effect of addition of an organic solvent on equilibrium constant K_V and, hence, also on pseudo-rate constant k_2 [see Eq. (25)], is expected to be of a lesser magnitude. In fact, whereas in the case of k_1 the effect is so notable (see Fig. 11, top) that it has been possible to correlate it with the number of carbon atoms in the hydrocarbon chain (see Fig. 12), in the

case of k_2 a clear-cut difference between the various organic solvents with an acceleration effect could not be established (see Fig. 11, bottom). The finding that 1-butanol had a decreasing effect on k_2, quite different from the effects produced by the other organic solvents, might be connected with its ability to aggregate in the form of micelles, thus introducing a big change in the medium structure.

The fact that the activation energy associated to the experimental rate constant k_1 is much lower than that associated to k_2 (87 ± 4 versus 120 ± 2 kJ mol^{-1}) is coherent with the fact that the intermediate $[Cr(H_2Y)(H_2O)_5]^+$ is long lived, since it must be formed in a fast step (low activation energy) and consumed in a slow step (high activation energy). In the opposite case, if it would have been formed in a slow step and consumed in a fast one, that species would behave as a short-lived intermediate in steady state, leading to continuously decreasing rate vs time plots, instead of the bell-shaped curves experimentally observed, as shown in Figs. 4 (top) and 6 (bottom). Moreover, the notable high values of the activation energies associated to both pseudo-rate constants is consistent with the well-known inherent kinetic inertness to substitution of the d^2sp^3 octahedral complexes of Cr(III) [46 – 48].

It should be noticed that, in the lack of any direct independent proof, the proposal of the formation of the 1:2 Cr(III)-EDTA complex in Eq. (21) should be considered as only a working hypothesis. Several indirect evidences of its existence, however, can be extracted from the present kinetic study: (i) The downward-concave curvature of the $A(540)_\infty$ vs $[Cr(III)]_o$ plot (Fig. 2, top), suggesting that at high [EDTA]/[Cr(III)] ratios a complex with a high molar absorption coefficient is predominantly formed (presumably, the 1:2 complex), whereas at low [EDTA]/[Cr(III)] ratios a complex with a low molar absorption coefficient is predominantly formed (the 1:1 complex). (ii) The finding that the final pH did not decrease monotonously as the metal ion initial concentration increased (situation expected if only 1:1

complexes were formed), since at high $[Cr(III)]_o$ values the plot showed a slight increase followed by a plateau (Fig. 2, bottom), suggesting that additional increases of $[Cr(III)]_o$ did not result in a further increase of the number of hydrogen ions released by EDTA to form the violet complex. (iii) The decrease of both H_{kin} and H_{th} as $[Cr(III)]_o$ increased (Fig. 7, top). (iv) The increase of both H_{kin} and H_{th} as $[EDTA]_o$ increased (Fig. 7, middle). (v) The increase of rate constant k_2 as $[EDTA]_o$ increased (Fig. 9, bottom), suggesting that the long-lived intermediate actually reacts with a second ligand molecule. Although the tendency of EDTA as a chelating ligand to wrap itself around a single metal center (thus leading to 1:1 complexes) is indeed well known, the rather prolonged lifetime of the long-lived intermediate (Fig. 6) might offer a chance for a second ligand molecule to become attached to Cr(III) before the first ligand molecule wraps itself around the metal center. This would be certainly consistent with the high activation energy associated to rate constant k_2, indicating that the conversion of the long-lived intermediate into the reaction product is notoriously slow.

Structures of the Cr(III)-EDTA Complexes

Given that Cr(III) forms hexacoordinated complexes and EDTA can behave as a hexadentate ligand (including two amine nitrogen atoms and four carboxylate oxygen atoms as electron donors), it might seem logic at first view that in the final violet complex six Cr(III)-EDTA bonds be involved. However, EDTA complexes with the organic ligand fully coordinated to the metal are known to present a considerable structural stress [28]. Consequently, there has been some discussion in the chemical literature on the actual number of Cr(III)-EDTA bonds involved in the violet complex, both in aqueous solution and in the solid state. Spectroscopic

studies have yielded apparently conflicting results. Some reports favor a structure with five bonds and the sixth metal position occupied by a water molecule, as proposed in the product $[Cr(HY)(H_2O)]$ formed in Eq. (23) [49 - 53]. Certainly, this structure agrees with the well-known fact that the Cr(III)-EDTA complex presents two distinct acidity equilibrium constants, corresponding to the loss of hydrogen ions from the unbounded carboxyl group of the organic ligand HY^{3-} and from the metal-bonded water molecule [29,54]. On the contrary, other reports favor a structure with six Cr(III)-EDTA bonds [28,29,55 – 57].

Since the sodium salt of the dianionic form of EDTA was used as organic reactant in the present study, if the predominant form of the final Cr(III)-EDTA complex was hexacoordinated, $[Cr(Y)]^-$, one would expect values of $H_{th} \approx 2$. However the experimental values were in most cases considerably lower. This finding suggests that the loss of the sixth water molecule from the coordination sphere of Cr(III) is very slow, probably involving a notably high activation energy:

$$[Cr(HY)(H_2O)] \rightleftharpoons [Cr(Y)(H_2O)]^- + H^+ \quad (27)$$

$$[Cr(Y)(H_2O)]^- \xrightarrow[\text{very slow}]{} [Cr(Y)]^- + H_2O \quad (28)$$

Eq. (27) suggests that an increase in the pH should result in a higher contribution of the hexacoordinated complex. This prediction agrees with the results shown in Fig. 7 (bottom), showing that at high $[KOH]_o$ the value of H_{th} approaches the theoretical limit of 2.

Applicability of the Kinetic Model

The procedure developed in this work for the treatment of the kinetic experimental data corresponding to the Cr(III)-EDTA reaction might prove useful for other complexation reactions involving as reactants aqua complexes of transition metal ions kinetically inert to substitution and different polydentate ligands.

BIBLIOGRAPHY

1. Perez-Benito, J. F.; Arias, C.; Rodriguez, R. M. J Phys Chem A 2001, 105, 1150 – 1157.
2. Bertoni, F. A.; Bellu, S. E.; Gonzalez, J. C.; Sala, L. F. Carbohydr Polym 2014, 114, 1 – 11.
3. Schwarz, K.; Mertz, W. Arch Biochem Biophys 1959, 85, 292 – 295.
4. Barrett, J.; O'Brien, P.; Pedrosa de Jesus, J. Polyhedron 1985, 4, 1 – 14.
5. Cooper, J. A.; Blackwell, L. F.; Buckley, P. D. Inorg Chim Acta 1984, 92, 23 – 31.
6. Kim, D. S.; Kim, T. W.; Kang, J. S. J. Trace Elem Med Biol 2004, 17, 243 – 247.
7. Dubois, F.; Belleville, F. Path Biol 1991, 39, 801 – 808.
8. McCarty, M. F. Med Hypotheses 1994, 43, 253 – 265.
9. Anderson, R. A. In Chromium and the Aging Process; Cser, M. A.; Laszlo, I. S.; Etienne, J. C.; Maymard, Y.; Centeno, J. A.; Khassanova, L.; Collery, P. Eds.; John Libbey Eurotext: Paris, France, 2004; Vol. 8.
10. El-Aila, H. J. Y. J Dispers Sci Technol 2012, 33, 1688 – 1694.
11. Liu, X.; Fan, J. H.; Ma, L. M. Water Air Soil Pollut 2013, 224, 1583.
12. Nash, K. L.; Brigham, D.; Shehee, T. C.; Martin, A. Dalton Trans 2012, 41, 14547 – 14556.

13. Evans, N.; Hallam, R. Mineral Mag 2012, 76, 3435 – 3438.
14. Broggs, M. A.; Islam, M.; Dong, W.; Wall, N. A. Radiochim Acta 2013, 101, 13 – 18.
15. Riha, M.; Karlickova, J.; Filipsky, T.; Macakova, K.; Hrdina, R.; Mladenka, P. J Inorg Biochem 2013, 123, 80 – 87.
16. Zhan, Y.; Chen, Y. W.; Lin, Z. X.; Li, Q.; Chen, Y. C.; Peng, L.; Han, M. Clin Lab 2014, 60, 543 – 551.
17. Choppin, G. R.; Thakur, P.; Mathur, J. N. Inorg Chim Acta 2017, 360, 1859 – 1869.
18. Garcia-Reyes, R. B.; Rangel-Mendez, J. R.; Alfaro-De la Torre, M. C. J Haz Mater 2009, 170, 845 – 854.
19. Thakur, P.; Xiong, Y. L.; Borkowski, M.; Choppin, G. R. Geochim Cosmochim Acta 2014, 133, 299 – 312.
20. Rush, J. D.; Koppenol, W. H. J Biol Chem 1986, 261, 6730 – 6733.
21. Rahhal, S.; Richter, H. W. J Am Chem Soc 1988, 110, 3126 – 3133.
22. Storkey, C.; Pattison, D. I.; Koehler, J. A.; Gaspard, D. S.; Evans, J. C.; Hagestuen, E. D.; Davies, M. J Food Chem 2015, 173, 645 – 651.
23. Armstrong, C.; Leong, W.; Less, G. J Brain Res 2001, 892, 51 – 62.
24. Stillhart, H.; Richterich, R.; Jeandet, J. Rev Int Hepat 1962, 12, 1125 – 1133.
25. Kontoghiorghes, G. J. Toxicol Mech Methods 2013, 23, 1 – 4.
26. Born, T.; Kontoghiorghe, C. N.; Spyrou, A.; Kolnagou, A.; Kontoghiorghes, G. J. Toxicol Mech Methods 2013, 23, 11 – 17.
27. Song, Y. Z.; Huang, Z. J.; Song, Y.; Tian, Q. J.; Liu, X. R.; She, Z. N.; Jiao, J.; Lu, E.; Deng, Y. H. Int J Nanomed 2014, 9, 3611 – 3621.
28. Wheeler, W. D.; Legg, J. I. Inorg Chem 1984, 23, 3798 – 3802.
29. Kanamori, K.; Kawai, K. Inorg Chem 1986, 25, 3711 – 3713.
30. Liu, B.; Chai, J.; Feng, S.; Yang, B. Spectrochim Acta A 2015, 140, 437 – 443.

31. Leupin, P.; Sykes, A. G.; Wieghardt, K. Inorg Chem 1983, 22, 1253 – 1254.

32. Balaska, F.; Bencheikh-Lehocine, M.; Chikhi, M.; Meniai, A. H. Energy Proc 2012, 19, 249 – 258.

33. Ogino, H.; Watanabe, T.; Tanaka, N. Inorg Chem 1975, 14, 2093 – 2097.

34. Ogino, H.; Shimura, M; Tanaka, N. Inorg Chem 1979, 18, 2497 – 2501.

35. Yamamoto, K.; Ohashi, K. Bull Chem Soc Jpn 1976, 9, 2433 – 2436.

36. Luo, Z.; Chatterjee, N. Chem Spec Bioavailab 2010, 22, 25 – 34.

37. Hamm, R. E. J Am Chem Soc 1953, 75, 5670 – 5672.

38. Hedrick, C. E. J Chem Educ 1965, 42, 479 – 480.

39. Barreto, J. C.; Brown, D.; Dubetz, T.; Kakareka, J.; Alberte, R. S. Chem Educator 2005, 10, 196 – 199.

40. Hecht, M.; Schultz, F. A.; Speiser, B. Inorg Chem 1996, 35, 5555 – 5563.

41. Espenson, J. H. Chemical Kinetics and Reaction Mechanisms; McGraw-Hill: New York, 1995.

42. Coetzee, J. F.; Ritchie, C. D. Solute-Solvent Interactions; Dekker: New York, 1969.

43. Perez-Benito, J. F.; Arias, C.; Rodriguez, R. M.; Ros, M. New J Chem 1998, 22, 1445 – 1451.

44. Perez-Benito, J. F. New J Chem 2001, 25, 268 – 274.

45. Robinson, P. J. J Chem Educ 1978, 55, 509 – 510.

46. Bakac, A.; Espenson, J. H. Acc Chem Res 1993, 26, 519 – 523.

47. Kornev, V. I.; Mikryukova, G. A. Russ J Coord Chem 2004, 30, 895 – 899.

48. Perez-Benito, J. F. J Trace Elem Med Biol 2006, 20, 161 – 170.

49. Brintzinger, H.; Thiele, H.; Muller, U. Z Anorg Allg Chem 1943, 251, 285 – 294.

50. Dwyer, F. P.; Garvan, F. L. J Am Chem Soc 1960, 82, 4823 – 4826.

51. Hoard, J. L.; Kenneard, C. H. L.; Smith, G. S. Inorg Chem 1963, 2, 1316 – 1317.

52. Thorneley, R. N. F.; Sykes, A. G. Chem Commun 1968, 340 – 341.

53. Gerdom, L. E.; Baenziger, N. A.; Goff, H. M. Inorg Chem 1981, 20, 1606 – 1609.

54. Knox, J. H.; Shibukawa, M. J Chromatogr 1991, 545, 123 – 134.

55. Sawyer, D. T.; McKinnie, J. M. J Am Chem Soc 1960, 82, 4191 – 4196.

56. Hoard, J. L.; Smith, G. S.; Lind, M. D. In Advances in the Chemistry of the Coordination Compounds; Kirschner, S. Ed.; Macmillan: New York, 1961.

57. Tsuchiya, R.; Uehara, A.; Kyuno, E. Bull Chem Soc Jpn 1969, 42, 1886 – 1891.

Table I Values of the Ratio of Molar Absorption Coefficients of the Long-Lived Intermediate and the Inorganic Reactant at 540 nm[a]

$[Cr(III)]_o$ (10^{-3} M)	$[EDTA]_o$ (10^{-2} M)	Q	E (10^{-4})
1.47	7.84	1.11 ± 0.05	4.14 ± 0.01
2.94	7.84	1.00 ± 0.04	3.71 ± 0.10
4.41	7.84	0.95 ± 0.02	4.52 ± 0.49
5.88	3.92	0.95 ± 0.01	4.41 ± 0.59
5.88	4.90	0.94 ± 0.03	3.95 ± 0.23
5.88	5.88	0.92 ± 0.02	5.36 ± 1.14
5.88	6.86	1.00 ± 0.01	3.92 ± 0.60
5.88	7.84	0.98 ± 0.03	3.84 ± 0.14
5.88	8.82	0.97 ± 0.05	3.50 ± 0.05
5.88	9.80	0.96 ± 0.02	4.02 ± 0.07
7.35	7.84	0.98 ± 0.02	3.76 ± 0.06
8.82	7.84	0.98 ± 0.01	5.97 ± 0.36
10.3	7.84	1.00 ± 0.02	4.71 ± 0.54
11.8	7.84	0.98 ± 0.01	8.94 ± 1.75

[a] E is the average error of the calculated absorbances with respect to the experimental values. Errors were calculated as one half of the range (2 determinations). Temperature: 25.0 ^oC.

Table II Kinetic Data at Various Initial Metal Ion Concentrations[a]

$[Cr(III)]_o$ (10^{-3} M)	k_1 (10^{-3} s^{-1})	k_2 (10^5 M^{-1} s^{-1})	H_{kin}	E (10^{-4})
1.47	1.45 ± 0.10	2.95 ± 0.05	1.572 ± 0.126	4.27 ± 0.13
2.94	1.43 ± 0.03	2.67 ± 0.01	1.201 ± 0.007	3.76 ± 0.09
4.41	1.53 ± 0.02	2.43 ± 0.04	0.975 ± 0.058	4.61 ± 0.57
5.88	1.39 ± 0.03	2.32 ± 0.06	0.782 ± 0.004	4.01 ± 0.30
7.35	1.49 ± 0.02	2.00 ± 0.03	0.686 ± 0.003	3.88 ± 0.06
8.82	1.54 ± 0.01	1.85 ± 0.03	0.583 ± 0.014	6.04 ± 0.31
10.3	1.46 ± 0.02	1.79 ± 0.01	0.484 ± 0.002	4.72 ± 0.54
11.8	1.63 ± 0.03	1.74 ± 0.05	0.393 ± 0.011	9.10 ± 1.73

[a] k_1 and k_2 are the pseudo-rate constants, H_{kin} the number of hydrogen ions released per Cr(III)-EDTA complex formed (kinetic value) and E the average error of the calculated absorbances with respect to the experimental values. Errors were calculated as one half of the range (2 determinations). Experimental conditions: $[Na_2EDTA]_o = 7.84 \times 10^{-2}$ M, 25.0 °C.

Table III Kinetic Data at Various Initial Potassium Nitrate Concentrations[a]

$[KNO_3]_o$ (M)	k_1 (10^{-3} s^{-1})	k_2 (10^5 M^{-1} s^{-1})	H_{kin}	E (10^{-4})
0.000	1.39 ± 0.03	2.32 ± 0.06	0.782 ± 0.004	4.01 ± 0.30
0.006	1.42 ± 0.03	2.23 ± 0.09	0.828 ± 0.046	3.31 ± 0.70
0.012	1.46 ± 0.04	2.23 ± 0.01	0.815 ± 0.013	3.49 ± 0.18
0.118	1.35 ± 0.10	2.29 ± 0.14	0.875 ± 0.048	3.54 ± 0.12
0.235	1.29 ± 0.03	2.37 ± 0.08	0.923 ± 0.014	3.78 ± 0.32
0.353	1.17 ± 0.04	2.47 ± 0.12	0.960 ± 0.029	3.76 ± 0.15
0.471	1.10 ± 0.01	2.62 ± 0.04	1.032 ± 0.001	3.66 ± 0.24
0.588	1.11 ± 0.01	2.79 ± 0.05	1.057 ± 0.031	4.04 ± 0.42

[a] k_1 and k_2 are the pseudo-rate constants, H_{kin} the number of hydrogen ions released per Cr(III)-EDTA complex formed (kinetic value) and E the average error of the calculated absorbances with respect to the experimental values. Errors were calculated as one half of the range (2 determinations). Experimental conditions: $[Cr(NO_3)_3]_o = 5.88 \times 10^{-3}$ M, $[Na_2EDTA]_o = 7.84 \times 10^{-2}$ M, 25.0 °C.

Table IV Effects of Various Organic Solvents on the Pseudo-Rate Constants[a]

Organic solvent	slope (k_1) (M^{-1})	slope (k_2) (M^{-1})
Methanol	0.031 ± 0.006	0.089 ± 0.004
Ethylene glycol	0.122 ± 0.015	0.115 ± 0.012
Ethanol	0.124 ± 0.006	0.081 ± 0.009
1-Propanol	0.191 ± 0.019	0.067 ± 0.008
2-Propanol	0.211 ± 0.013	0.071 ± 0.008
Acetone	0.263 ± 0.016	0.083 ± 0.012
1-Butanol	0.351 ± 0.020	-0.113 ± 0.010

[a] The slopes correspond to the log ($k_1/k_{1,0}$) vs [organic solvent]$_o$ and log ($k_2/k_{2,0}$) vs [organic solvent]$_o$ linear plots. Errors were calculated as the statistical standard deviations of the slopes. Experimental conditions: $[Cr(NO_3)_3]_o = 5.88 \times 10^{-3}$ M, $[Na_2EDTA]_o = 3.92 \times 10^{-2}$ M, 25.0 ^oC.

Table V Activation Parameters Associated to the Pseudo-Rate Constants[a]

Activation parameter	k_1	k_2
$\ln A$	29 ± 2	61 ± 1
E_a (kJ mol^{-1})	87 ± 4	120 ± 2
$\Delta H^{o}_{\neq}$ (kJ mol^{-1})	84 ± 4	118 ± 2
$\Delta S^{o}_{\neq}$ (J K^{-1} mol^{-1})	-15 ± 15	252 ± 7

[a] The Arrhenius pre-exponential factors (A) are given in either s^{-1} (k_1) or M^{-1} s^{-1} (k_2). Errors associated to the activation parameters were calculated from the standard deviations for the intercept and slope of the Arrhenius and Eyring plots. The activation entropies are referred to the 1 M standard state. Experimental conditions: $[Cr(NO_3)_3]_o = 5.88 \times 10^{-3}$ M, $[Na_2EDTA]_o = 9.80 \times 10^{-2}$ M, 20.0 – 30.0 ºC.

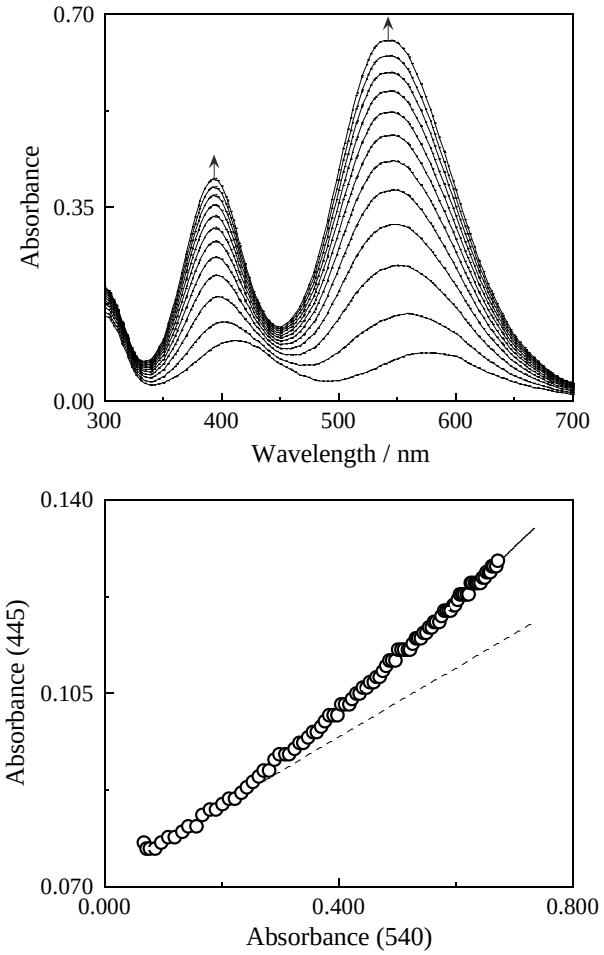

Figure 1 Periodical scanning of the UV-Vis spectrum recorded at 32-min intervals (top) and absorbance at 445 nm as a function of the absorbance at 540 nm measured periodically at 4-min intervals (bottom) during the course of the reaction at $[Cr(NO_3)_3]_o = 5.88 \times 10^{-3}$ M, $[Na_2EDTA]_o = 8.82 \times 10^{-2}$ M and 25.0 ºC. The arrows show the progression of the reaction. The dashed line is the tangent to the curve at time zero.

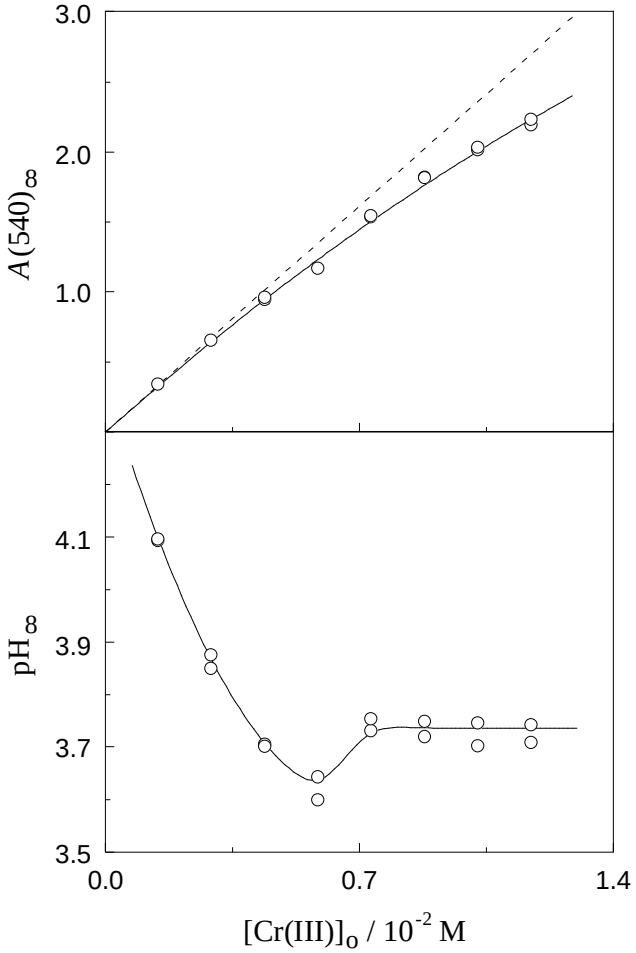

Figure 2 Final absorbance at 540 nm (top) and pH (bottom) as a function of the initial metal ion concentration at $[Na_2EDTA]_o = 7.84 \times 10^{-2}$ M and 25.0 ºC. The dashed line is the tangent to the curve at $[Cr(III)]_o = 0$.

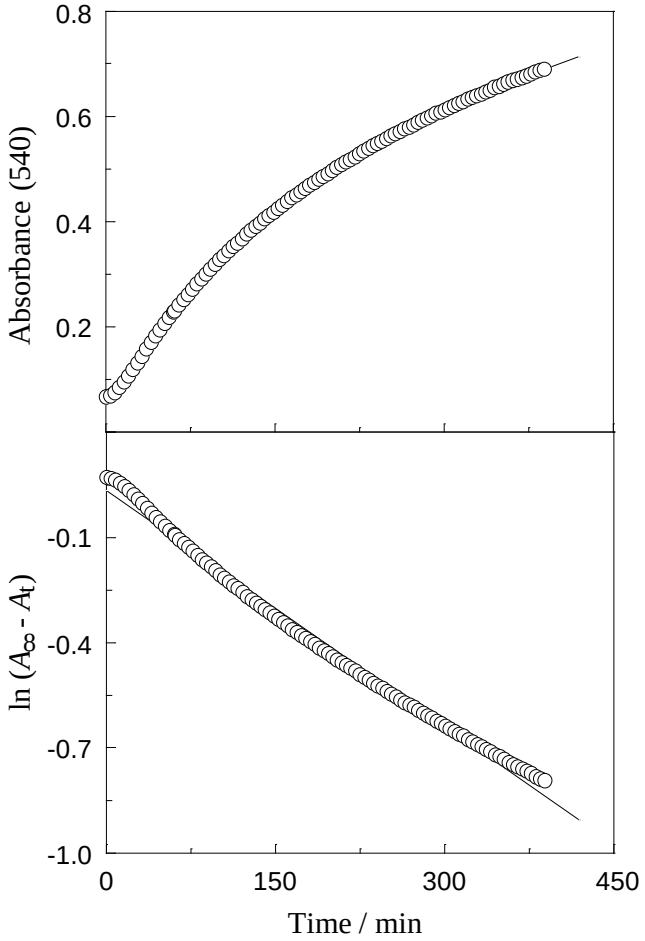

Figure 3 Absorbance at 540 nm as a function of time measured periodically at 4-min intervals during the course of the reaction (top) and attempted pseudo-first-order plot (bottom) at $[Cr(NO_3)_3]_o = 5.88 \times 10^{-3}$ M, $[Na_2EDTA]_o = 9.80 \times 10^{-2}$ M and 25.0 ºC.

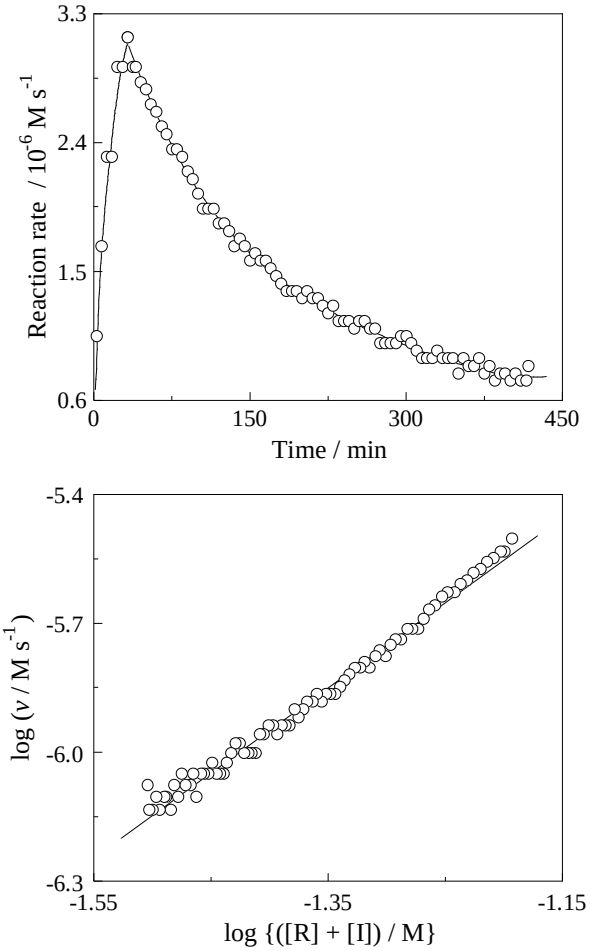

Figure 4 Reaction rate as a function of time (top) and double-logarithm plot of the reaction rate against the total concentration of limiting reactant and long-lived intermediate for the deceleration period (bottom) at $[Cr(NO_3)_3]_o = 5.88 \times 10^{-3}$ M, $[Na_2EDTA]_o = 6.86 \times 10^{-2}$ M and 25.0 ºC.

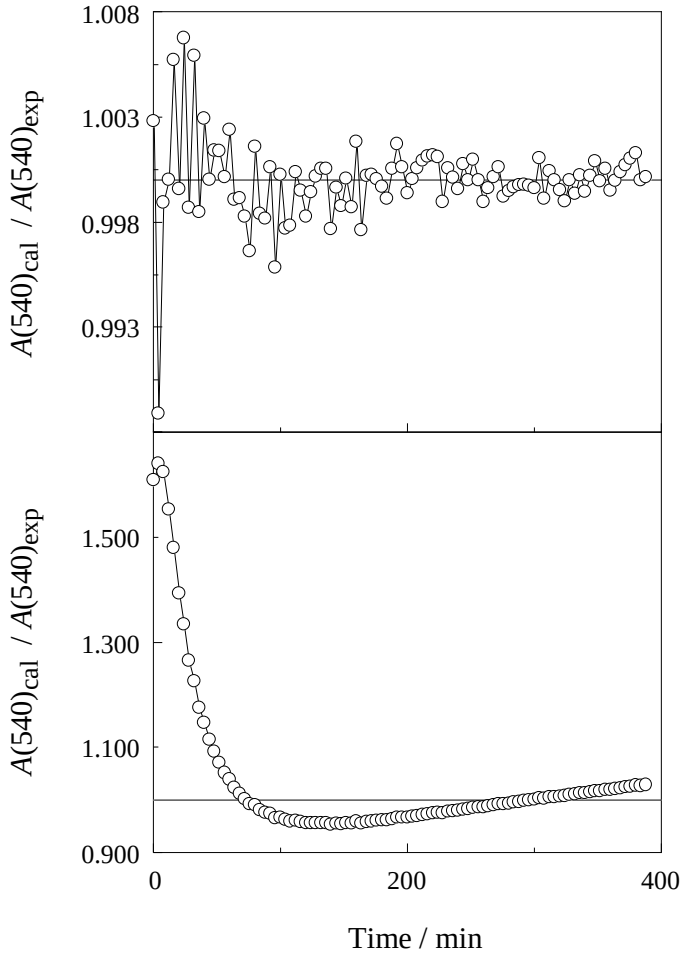

Figure 5 Ratio between the calculated and experimental values of the absorbance at 540 nm as a function of time at 4-min intervals for the one rate-constant (bottom, $E = 1.43 \times 10^{-2}$) and two rate-constant (top, $E = 3.45 \times 10^{-4}$) kinetic models with $[Cr(NO_3)_3]_o = 5.88 \times 10^{-3}$ M, $[Na_2EDTA]_o = 8.82 \times 10^{-2}$ M and 25.0 ºC.

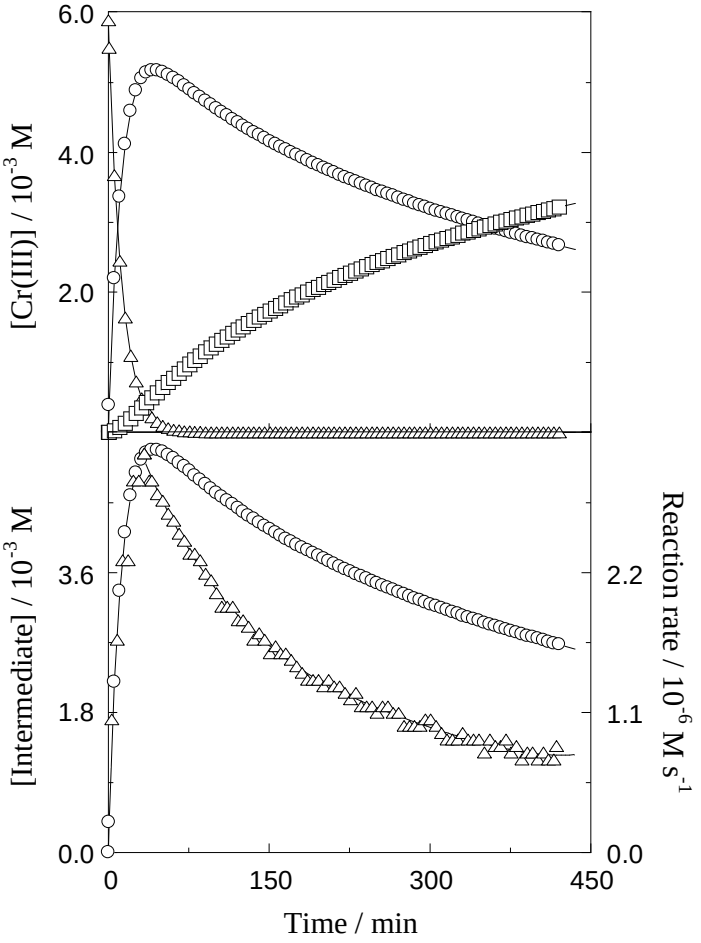

Figure 6 Top: concentrations of three Cr(III) species [reactant (triangles), long-lived intermediate (circles) and product (squares)] according to the two rate-constant kinetic model as a function of time. Bottom: comparison between the experimental values of the reaction rate (triangles) and the calculated long-lived intermediate concentration (circles) as a function of time. $[Cr(NO_3)_3]_o = 5.88 \times 10^{-3}$ M, $[Na_2EDTA]_o = 6.86 \times 10^{-2}$ M and 25.0 ºC.

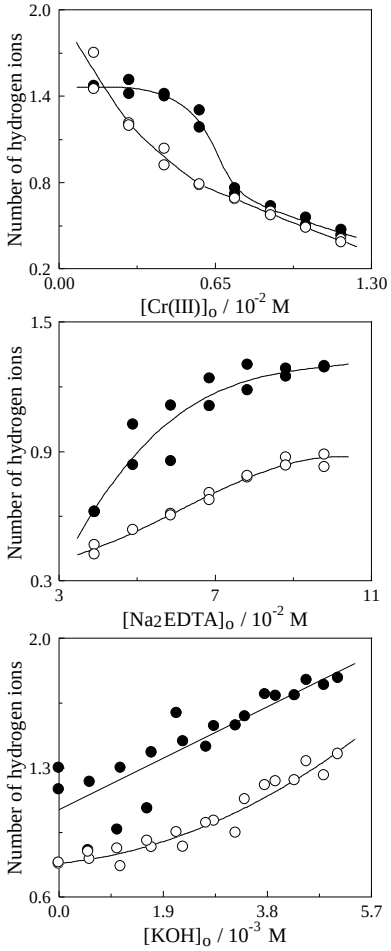

Figure 7 Number of hydrogen ions released per Cr(III)-EDTA complex molecule formed at 25.0 ºC as a function of the initial concentration of: metal ion (top, $[Na_2EDTA]_o = 7.84 \times 10^{-2}$ M), organic ligand (middle, $[Cr(NO_3)_3]_o = 5.88 \times 10^{-3}$ M) and potassium hydroxide (bottom, $[Cr(NO_3)_3]_o = 5.88 \times 10^{-3}$ M and $[Na_2EDTA]_o = 7.84 \times 10^{-2}$ M). Empty circles: kinetic values obtained from the fitting of the absorbance-time data by numerical simulations (H_{kin}). Filled circles: thermodynamic values obtained from the final pH measurements (H_{th}).

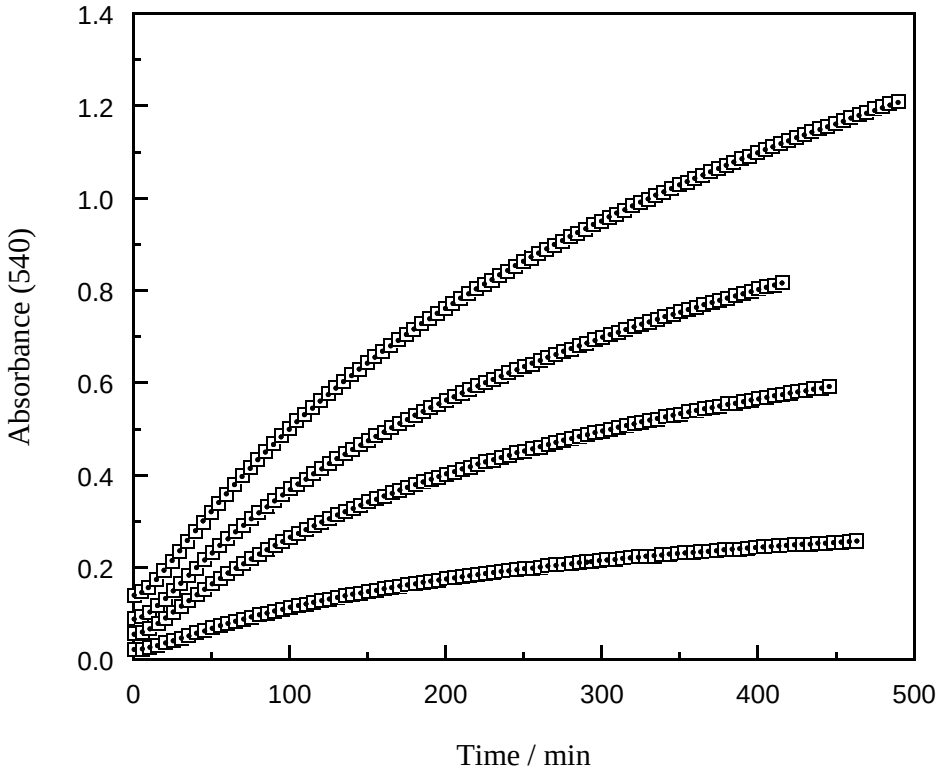

Figure 8 Absorbance at 540 nm as a function of time measured periodically at 5-min intervals during the course of the reaction at $[Cr(NO_3)_3]_o$ = 1.47, 4.41, 7.35 and 11.8 (from bottom to top) $\times 10^{-3}$ M, $[Na_2EDTA]_o = 7.84 \times 10^{-2}$ M and 25.0 ºC. Squares: Experimental absorbances. Black points inside: Theoretical absorbances predicted by the two rate-constant kinetic model.

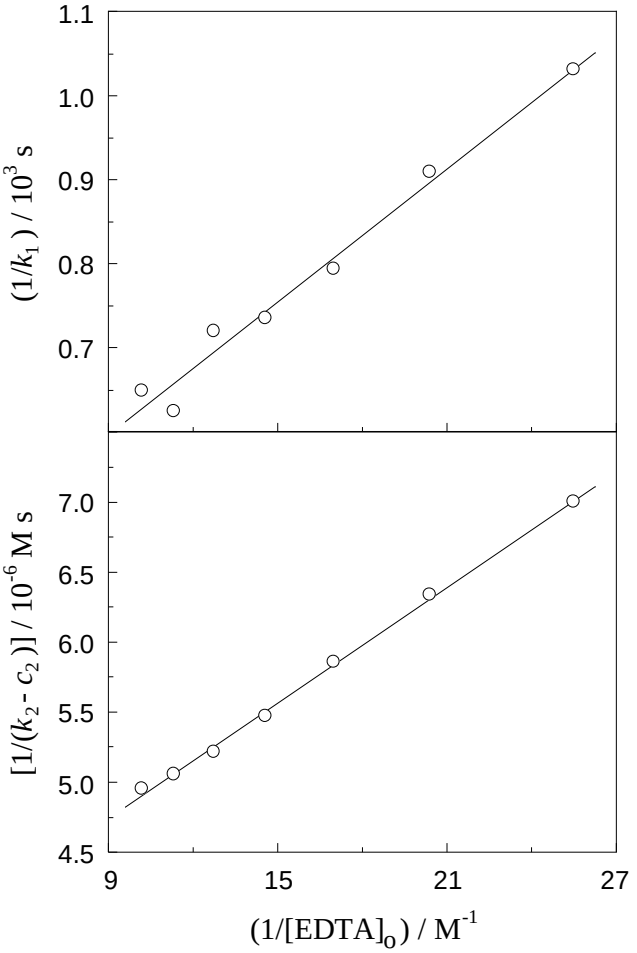

Figure 9 Dependences of the pseudo-rate constants k_1 (top) and k_2 (bottom) on the initial organic ligand concentration at $[Cr(NO_3)_3]_o$ = 5.88×10^{-3} M, $[Na_2EDTA]_o$ = $(3.92 - 9.80) \times 10^{-2}$ M and 25.0 ºC.

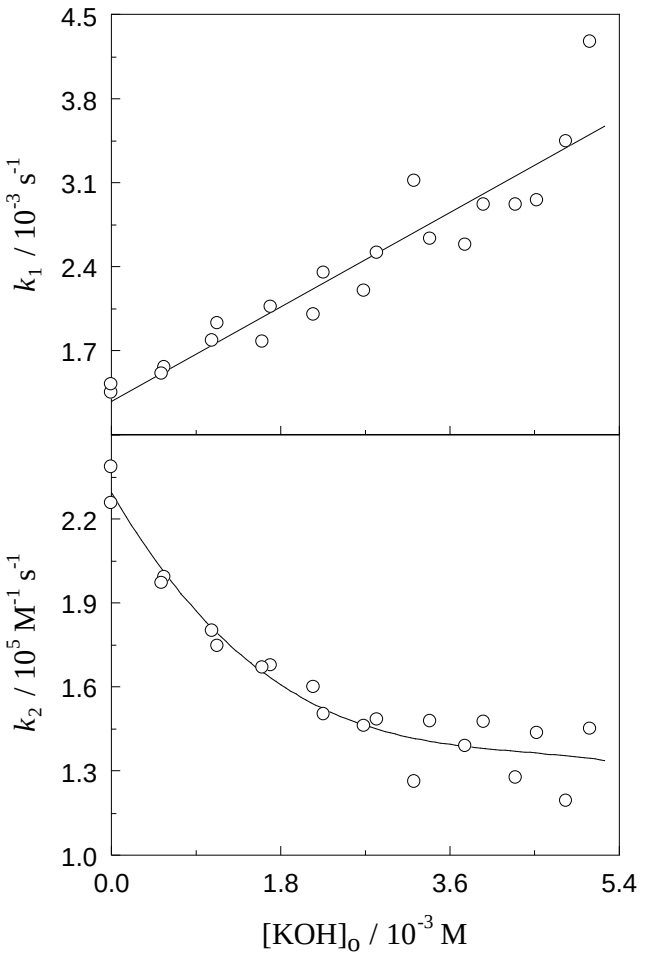

Figure 10 Dependences of the pseudo-rate constants k_1 (top) and k_2 (bottom) on the initial potassium hydroxide concentration at $[Cr(NO_3)_3]_o = 5.88 \times 10^{-3}$ M, $[Na_2EDTA]_o = 7.84 \times 10^{-2}$ M and 25.0 ºC.

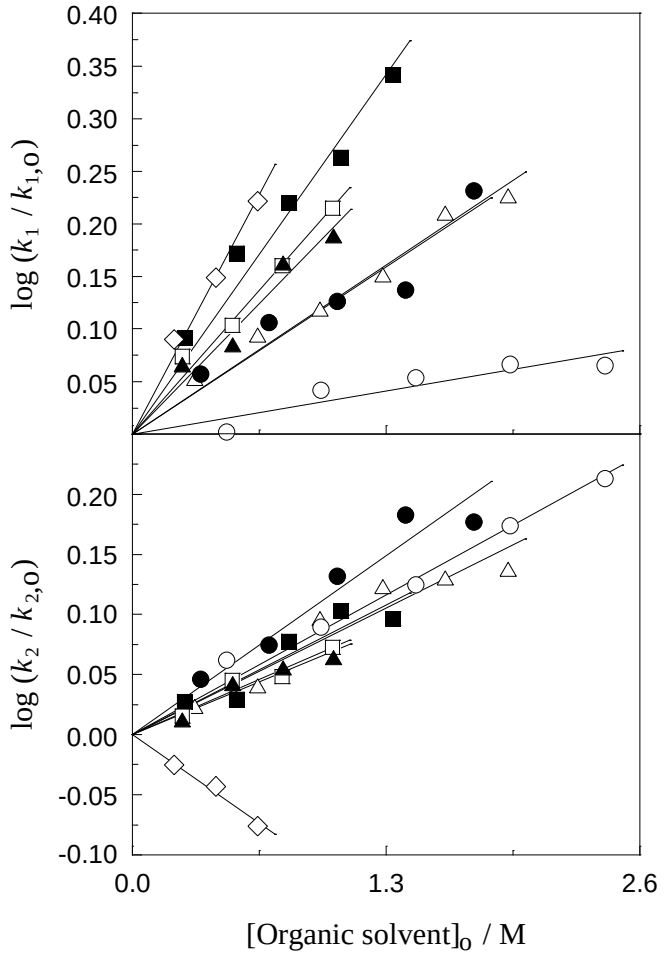

Figure 11 Dependences of the logarithms of the ratios of the pseudo-rate constants k_1 (top) and k_2 (bottom) in the presence and absence ($k_{1,0}$ and $k_{2,0}$) of added organic solvent on the initial concentrations of methanol (empty circles), ethylene glycol (filled circles), ethanol (empty triangles), 1-propanol (filled triangles), 2-propanol (empty squares), acetone (filled squares) and 1-butanol (rhombuses) at $[Cr(NO_3)_3]_o = 5.88 \times 10^{-3}$ M, $[Na_2EDTA]_o = 3.92 \times 10^{-2}$ M and 25.0 ºC.

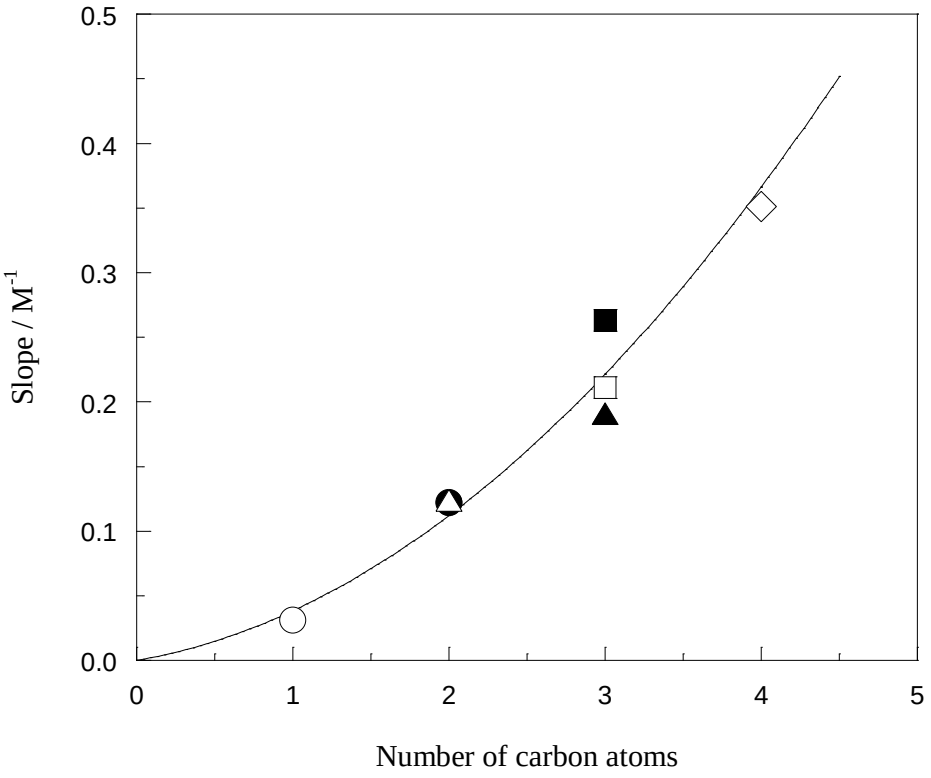

Figure 12 Dependence of the slope corresponding to the log ($k_1/k_{1,0}$) vs [organic solvent]$_o$ linear plot ($k_{1,0}$ being the pseudo-rate constant in the absence of organic solvent) on the number of carbon atoms in the hydrocarbon chain. Solvents: methanol (empty circle), ethylene glycol (filled circle), ethanol (empty triangle), 1-propanol (filled triangle), 2-propanol (empty square), acetone (filled square) and 1-butanol (rhombus). Experimental conditions: $[Cr(NO_3)_3]_o = 5.88 \times 10^{-3}$ M, $[Na_2EDTA]_o = 3.92 \times 10^{-2}$ M and 25.0 ºC.

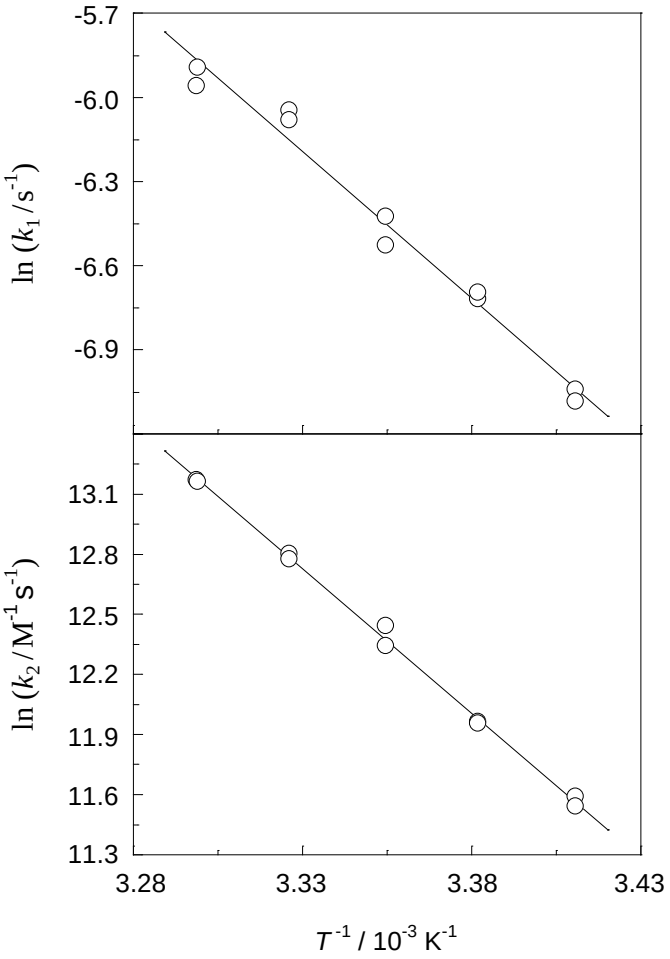

Figure 13 Arrhenius plots for the pseudo-rate constants k_1 (top) and k_2 (bottom) at $[Cr(NO_3)_3]_o = 5.88 \times 10^{-3}$ M, $[Na_2EDTA]_o = 9.80 \times 10^{-2}$ M and 20.0 – 30.0 ºC.